# Spectral Computed Tomography Findings of Peripheral Lung Adenocarcinoma and Peripheral Squamous Cell Carcinoma

**Liangna Deng**
Lanzhou University Second Hospital
**Guojing Zhang**
Lanzhou University Second Hospital
**Xiaoqiang Lin**
Lanzhou University Second Hospital
**Mengyuan Jing**
Lanzhou University Second Hospital
**Tao Han**
Lanzhou University Second Hospital
**Bin Zhang**
Lanzhou University Second Hospital
**Junlin Zhou** ( lzuzjl601@163.com )
Lanzhou University https://orcid.org/0000-0003-0036-6670

**Research article**

**Keywords:** Spectral CT, lung cancer, lung squamous cell carcinoma, lung adenocarcinoma, diagnosis

**Posted Date:** December 21st, 2020

**DOI:** https://doi.org/10.21203/rs.3.rs-131031/v1

# Abstract

**Background:** To investigate the spectral computed tomography (CT) findings of peripheral adenocarcinoma (P-AC) and peripheral squamous cell carcinoma (P-SCC) in lung.

**Methods:** In this retrospective study, A total of 273 patients (150 patients with P-AC and 123 patients with P-SCC) confirmed by surgery and pathology who underwent chest contrast enhanced CT scan with GSI mode, including arterial phase (AP) and venous phase (VP). During two phases, The $CT_{40keV}$, $CT_{70keV}$, $CT_{100keV}$ values, iodine concentration (IC), water concentration (WC), effective atomic number (Zeff) were measured and the slope of the spectral curve (K) was calculated. Differences between two groups were compared using two-sample t-test, Receiver operating characteristic (ROC) curves were plotted, and the area under the ROC curve (AUC) was also calculated to calculate diagnostic efficacies.

**Results**: There was significant difference in gender between the two groups ($P < 0.05$), No significant difference between other clinical features and symptoms ($P > 0.05$). For AP and VP, the $CT_{40keV}$, $CT_{70keV}$, $K70_{keV}$, IC and Zeff of P-AC were significantly higher than those of P-SCC ($P<0.05$), but there was no significant difference in WC and CT100keV between the two groups. ROC curve analysis showed that the combination of all quantitative parameters in AP and VP had the best diagnostic performance, with the area under the curve, sensitivity and specificity of 92%, 88%, and 84%, respectively.

**Conclusions**: Spectral CT can provide reference for the differentiation of P-AC and P-SCC.


# Background

Lung cancer is one of the malignant tumors with the highest morbidity and mortality in the world [1]. With the increase of the aging population, the incidence of lung cancer is also on the rise. Non-small cell lung cancer accounts for about 85% of all lung cancer cases, adenocarcinoma (AC) and squamous cell carcinoma (SCC) are the two most common histological types of non-small cell lung cancer [2]. AC and SCC have different histopathological characteristics, biological characteristics and clinical treatment methods [3, 4]. According to the anatomical location of the disease, lung cancer is divided into the central lung cancer and peripheral lung cancer. lung cancer can be divided into central type and peripheral type. SCC mainly occurs in the proximal airway, mainly in the central type, while AC mainly occurs in the distal airway, mainly in the peripheral type [5]. At present, the pathological types of lung cancer are determined by fine-needle aspiration biopsy, bronchoscopy, cytological examination or surgery to obtain tumor tissue [6]. However, these are invasive methods of examination, when some tumors are close to the bone or located deep, it is difficult to obtain tumor tissue [7], and biopsies can increase the risk of tumor metastasis [8].In addition, the early clinical symptoms of peripheral lung cancer are not obvious. Symptoms only appear as the disease progresses or metastasis occurs. At this time, most patients are in the middle and advanced stages of lung cancer and have lost the opportunity of surgical resection [9]. Therefore, it is necessary to identify subtypes of lung cancer in a non-invasive and easy-to-operate way.

Computed tomography (CT) is the preferred imaging method for early screening, diagnosis and stage assessment of lung cancer at present. Some studies have used traditional CT to distinguish peripheral adenocarcinoma (P-AC) from peripheral squamous cell carcinoma (P-SCC) [10–13]. For example, Yue and colleagues found that deep lobulated margins, thickened vascular bundles and pleural indentation are more common in AC, while smooth margins and bronchiectasis are more common in SCC [10]. Jiang et al. [13] studied the thin-slice CT findings of peripheral lung cancer below 3 cm, and found that the incidence of air bronchogram sign in P-AC was significantly higher than that in P-SCC, and the difference was statistically significant ($P < 0.05$). Kunihiro et al. [12] compared the CT findings of AC and SCC, and found that the maximum thickness of the cavity wall of AC was smaller than that of SCC and ground-glass shadow and bronchiectasis were more common in AC. However, the CT signs selected in these studies are easily affected by the subjective judgment of the observer; in addition, the results of these studies are contradictory. Traditional CT can only provide some information about the morphological characteristics of the lesions and the relationship between the lesions and adjacent tissues, while the information for the identification of pathological subtypes of lung cancer is limited [14, 15].

In recent years, with the development of energy imaging technology and the increase of clinical demand, the research of energy CT has become a hot spot, especially the spectral CT imaging that appeared in 2009, which provides a broader space for the research and clinical application of energy imaging [16, 17]. Dual-energy spectral CT uses instantaneous kVp switching technology, which can provide material density images and single energy images, and perform multi-parameter quantitative analysis on the histological and biological characteristics of the lesions [17]. Compared with traditional CT, it has more advantages in distinguishing benign and malignant lung lesions and pathological grade of lung cancer [18, 19]. The purpose of this study is to investigate the spectral CT findings of P-AC and P-SCC and to provide a reference for the differential diagnosis of them.

## Methods

# Study population

This study retrospectively analyzed data from 273 patients (160 males, 113 females; mean ± standard deviation [SD] age, 63.89 ± 9.32 years; range, 36–78 years) who were diagnosed with peripheral lung cancer confirmed by pathology in our hospital between January 2014 to August 2020, including 123 patients (92 males, 51 females, range, 43–78 years, mean ± SD age, 65.23 ± 10.73 years) with P-SCC and 150 patients (68 males, 82 females, range, 36–72 years, mean ± SD age, 62.56 ± 8.89 years) with P-AC. Inclusion criteria: (1) not receiving any anti-tumor treatment before spectral CT scan; (2) no history of hypersensitivity or contraindications to iodine contrast agent; (3) the time interval between operation and spectral CT scan is within 2 weeks; (4) the patients are over 18 years old; (5) it was confirmed by histopathology. Exclusion criteria: (1) CT scan showed that the tumor is located in the center; (2) the area of necrosis or calcification exceeded 50% of the tumor volume; (3) the tumor volume was too small to affect the measurement results; (4) there is heavy breathing artifacts or poor image quality. All patients signed an informed consent form before CT scan.

# Ct Imaging Techniques

All patients underwent CT examinations with GSI mode using Discovery CT750 HD (GE Healthcare, Waukesha, WI, USA) scanner. Scanning range: the entrance of thorax to the level of costophrenic angle. Scanning parameters: tube voltage: high and low energy (80kVp, 140 kVp) instantaneous (0.5 ms) switching, tube current 375 mA, tube rotation time 0.7 s, screw pitch, 0.984:1; scanning field of view, 50 cm; collimator width, 40 mm; scanning layer thickness and spacing are 5 mm. Then a bolus of 80 ~ 100 ml (1.2 mL/kg body weight) of non-ionic contrast media (Ultravist 300, Bayer Pharma, Berlin, Germany) was injected into the median cubital vein at a rate of 3.5 ~ 4 ml/s. The arterial phase (AP) and venous phase (VP) scanning were performed in GSI mode for 30 s and 60 s after contrast medium injection, respectively. The CT images of AP and VP are reconstructed with a layer thickness and spacing of 1.25 mm, Adaptive iterative reconstruction (ASIR) algorithm is used to reduce the noise of the image.

# Radiological Diagnoses

Two radiologists with 10 years of experience in thoracic tumor diagnosis blindly used the GSI Viewer analysis software in the GE AW4.6 workstation to independently analyze the images, and reached an agreement after discussion in the case of differences. Select the largest layer of the lesion and its adjacent upper and lower layers to measure the region of interest (ROI) in three consecutive layers. In order to reflect the heterogeneity of the tumor as much as possible, when the density of the lesion is uniform, the area of the ROI should be larger than the cross-section of the lesion 1/2 of the surface. When the density of the lesion is uneven, the area with more solid components and uniform enhancement should be selected as much as possible. At the same time, in order to maintain the accuracy of the measurements, copy and paste functions are used to ensure that the ROI is consistent in size, shape, and location during the arterial and venous phases. An elliptical region of interest was placed in the area where should avoid the areas of blood vessels, calcification, cavitation, necrotic cystic, atelectasis and so on. Each lesion is measured three times and the average value is calculated, and then the average value measured by two radiologists was calculated again. GSI Viewer software automatically generates the CT value, iodine concentration (IC), water concentration (WC) and effective atomic number (Zeff) under single energy of 40–100 keV (interval 10 keV), and calculates the slope of the spectral curve, According to the equation:

$K_{70\ keV} = (CT_{40\ keV} - CT_{70\ keV}) / (70 - 40)$.

# Statistical analysis

Statistical analysis was performed using SPSS version 22.0 (IBM Corporation, Armonk, NY, USA). The quantitative parameters were expressed as mean ± standard deviation and the counting data as percentage. The differences in gender, smoking history and clinical characteristics between the two groups were compared using the $\chi^2$ test. the differences between the two groups in age and quantitative

parameters were statistically compared using the two-sample t-test; The ROC curve was drawn for the above variables with statistical differences, and calculated the area under the ROC curve, sensitivity, specificity, maximum Youden index and optimal threshold.

# Results

There were 92 males (74.7%) and 31 females (25.3%) with P-SCC and 68 males (45.3%) and 82 females (54.7%) with P-AC. there was statistical significance between the two groups in terms of gender ($P < 0.001$). There was no significant difference in age, smoking history and clinical symptoms between the two groups ($P > 0.05$) (Table 1).

Table 1
Demographic and clinical characteristics of peripheral squamous cell carcinoma and peripheral adenocarcinoma

| Variable | P-SCC (n = 123) | P-AC (n = 150) | $\chi^2/t$ | *P* |
|---|---|---|---|---|
| Age(years) | | | -0.09 | 0.09 |
| Mean ± SD | 59.81 ± 8.01 | 58.05 ± 8.80 | | |
| Median/Range | 60(43–79) | 57(29–78) | | |
| Sex(%) | | | 59.19 | 0.05 |
| Male | 102(82.93) | 55(36.67) | | |
| Female | 21(17.07) | 95(63.33) | | |
| Smoking history (%) * | | | 0.28 | 0.6 |
| Yes | 72(58.5) | 83(55.3) | | |
| No | 51(41.5) | 67(44.7) | | |
| Symptom(%) | | | 0.89 | 0.93 |
| Asymptoms | 26(21.1) | 28(18.7) | | |
| Cough | 42(34.1) | 55(36.6) | | |
| Hemoptysis | 31(25.2) | 34(22.7) | | |
| Chest pain | 18(14.6) | 26(17.3) | | |
| Dyspnea | 14(11.3) | 19(12.7) | | |

P-AC, peripheral lung adenocarcinoma; P-SCC, peripheral lung squamous cell carcinoma; SD: Standard deviation; *Smoking history is defined as follows, Yes, former and current smokers; No, never smoked.

In the AP and VP, the $CT_{40keV}$, $CT_{70keV}$, $K_{70keV}$, IC and Zeff of P-AC were greater than those of S-CC, and the difference was statistically significant ($P < 0.001$), while the WC and $CT_{100keV}$ between the two groups were not statistically significant (Table 2). The examples of P-SCC and P-AC are presented in Figs. 1 and 2.

Table 2
Comparison of spectral quantitative parameters of peripheral squamous cell carcinoma and peripheral adenocarcinoma in the arterial and venous phases

| | P-SCC (n = 123) | P-AC (n = 150) | *t* | *P* |
|---|---|---|---|---|
| **AP** | | | | |
| $CT_{40keV}$ (HU) | 147.68 ± 11.08 | 164.24 ± 11.83 | 11.83 | < 0.001 |
| $CT_{70keV}$ (HU) | 66.04 ± 6.75 | 69.31 ± 7.52 | 3.74 | < 0.001 |
| $CT_{100keV}$ (HU) | 46.18 ± 6.98 | 47.47 ± 8.32 | 1.4 | 0.16 |
| $K_{70keV}$ | 2.72 ± 0.31 | 3.16 ± 0.36 | 10.94 | < 0.001 |
| IC (100 μg/cm$^3$) | 8.46 ± 0.09 | 8.57 ± 0.11 | 9.23 | < 0.001 |
| Zeff | 14.31 ± 1.66 | 16.42 ± 1.94 | 9.66 | < 0.001 |
| WC (mg/cm$^3$) | 1,029.95 ± 7.92 | 1,028.50 ± 10.21 | −1.32 | 0.19 |
| **VP** | | | | |
| $CT_{40keV}$ (HU) | 124.26 ± 14.52 | 134.45 ± 10.87 | 6.44 | < 0.001 |
| $CT_{70keV}$ (HU) | 56.03 ± 7.02 | 58.35 ± 5.86 | 2.97 | 0.03 |
| $CT_{100keV}$ (HU) | 39.48 ± 6.80 | 40.61 ± 6.10 | 1.46 | 0.15 |
| $K_{70keV}$ | 2.27 ± 0.41 | 2.53 ± 0.33 | 5.71 | < 0.001 |
| IC (100 μg/cm$^3$) | 8.32 ± 0.12 | 8.39 ± 0.10 | 5.12 | < 0.001 |
| Zeff | 11.92 ± 2.14 | 13.19 ± 1.75 | 5.28 | < 0.001 |
| WC (mg/cm$^3$) | 1,025.94 ± 7.89 | 1,025.65 ± 7.31 | −0.32 | 0.74 |

AP: Arterial phase; HU, Hounsfield; IC, iodine concentration; P-AC, peripheral lung adenocarcinoma; P-SCC, peripheral lung squamous cell carcinoma; VP: Venous phase; WC, water concentration; Zeff, effective atomic number.

The ROC analysis results of spectral CT quantitative parameters of the AP and VP energy spectrum are presented in Table 3 and Fig. 3. The analysis shows that in AP, the area under the ROC curve of $CT_{40keV}$ (0.84), $K_{70keV}$ (0.83), Zeff (0.80), and the combination of quantitative parameters of the AP (0.87) are all

≥ 0.8, and the area under the ROC curve of the combination of quantitative parameters of the AP was the largest (0.87). In the venous phase, only the area under the ROC curve of the combination of quantitative parameters was ≥ 0.75, and the area under the ROC curve of $CT_{40keV}$ (0.73) and $K_{70keV}$ (0.71) was ≥ 0.7. The area under the ROC curve of the combination of all quantitative parameters in AP and VP was 0.92, which was the largest among all the parameters in AP and VP.

Table 3
ROC curve analysis of CT quantitative parameters of peripheral squamous cell carcinoma and peripheral adenocarcinoma

| Parameter | AUC(95%CI) | YI | Threshold | Sensitivity (%) | Specificity (%) |
|---|---|---|---|---|---|
| **AP** | | | | | |
| $CT_{40keV}$ (HU) | 0.84(0.80–0.89) | 0.61 | 153.83 | 0.82 | 0.8 |
| $CT_{70keV}$ (HU) | 0.64(0.57–0.70) | 0.25 | 69.67 | 0.51 | 0.73 |
| $K_{70keV}$ | 0.83(0.78–0.88) | 0.55 | 2.91 | 0.77 | 0.78 |
| IC (100 μg/$cm^3$) | 0.79(0.74–0.85) | 0.48 | 14.94 | 0.79 | 0.68 |
| Zeff | 0.80(0.75–0.85) | 0.47 | 14.94 | 0.79 | 0.68 |
| AP-all | 0.87(0.85–0.93) | 0.67 | 0.44 | 0.84 | 0.84 |
| **VP** | | | | | |
| $CT_{40keV}$ (HU) | 0.72(0.66–0.79) | 0.48 | 124.49 | 0.85 | 0.63 |
| $CT_{70keV}$ (HU) | 0.63(0.56–0.70) | 0.25 | 57.35 | 0.61 | 0.63 |
| $K_{70keV}$ | 0.71(0.64–0.77) | 0.36 | 0.69 | 0.69 | 0.68 |
| IC (100 μg/$cm^3$) | 0.69(0.62–0.75) | 0.33 | 8.36 | 0.7 | 0.62 |
| Zeff | 0.69(0.63–0.76) | 0.36 | 12.57 | 0.7 | 0.65 |
| VP-all | 0.75(0.69–0.81) | 0.51 | 0.56 | 0.62 | 0.89 |
| **AP-all + VP-all** | 0.92(0.89–0.95) | 0.72 | 0.41 | 0.88 | 0.84 |

AP, Arterial phase; AP-all, AP ($CT_{40keV}$ + $CT_{70keV}$ + $K_{70keV}$ + IC + Zeff); AP-all + VP-all, AP ($CT_{40keV}$ + $CT_{70keV}$ + $K_{70keV}$ + IC + Zeff) + VP ($CT_{40keV}$ + $CT_{70keV}$ + $K_{70keV}$ + IC + Zeff); AUC, Area under cure; IC, Iodine concentration; VP, Venous phase; VP-all, VP ($CT_{40keV}$ + $CT_{70keV}$ + $K_{70keV}$ + IC + Zeff); YI, Youden index; Zeff, Effective atomic number.

ROC curve analysis was used to determine the optimal threshold for the sensitivity and specificity of differentiating P-SCC and P-AC. For example, during Ap, when $CT_{40keV}$ threshold was 153.83, the sensitivity and specificity of differentiating P-SCC and P-AC were 0.82 and 0.80, respectively. At the

venous stage, the threshold value of $CT_{40keV}$ was 124.49, and the sensitivity and specificity were 0.85 and 0.63, respectively. For the selected combination of optimal thresholds, the optimal threshold for distinguishing between P-AC and P-SCC were the combination of all combined quantitative parameters in AP and VP of 0.41, and the sensitivity and specificity were 0.88 and 0.84, respectively.

# Discussion

With the development of personalized medicine and molecular targeting therapy, it is particularly important to determine the pathological type of lung cancer before starting treatment, because the efficacy of targeted drugs depends on the pathological subtype of lung cancer, For example, such as bevacizumab are effective in the treatment of AC, but it may lead to neutropenia and massive bleeding in patients with SCC [20, 21]. The diagnostic accuracy of peripheral lung squamous cell carcinoma and peripheral lung adenocarcinoma is very limited due to the overlap of imaging signs on conventional CT. The multi-parameter of spectral CT can effectively reflect the tissue composition and biological characteristics of the tumor, and has great potential in identifying tumor subtypes and differentiation degree [17]. Wang et al. [22] studied the spectral CT manifestations of AC and SCC and found that spectral CT can provide both qualitative and quantitative parameters of the lesion, which provides a new method for differentiating them.

In this study, we found that $CT_{40keV}$, $CT_{70keV}$, $K_{70keV}$ and IC in patients with P-AC in both AP and VP were higher than those in patients with P-SCC, which was consistent with the results of previous studies [23–25], indicating that the blood supply of AC was more abundant than that of SCC. According to the results of previous pathological studies [26], the capillary endothelial cells in normal tissues are tightly connected and the basement membrane is intact, and the contrast agent rarely penetrates into the intercellular space. However, a large number of new capillaries are formed in the tumor tissue, in which the capillary endothelial cells are loosely connected and the basement membrane is incomplete, so the contrast agent can easily penetrate into the intercellular space. Yazdani et al. [27] found that compared with SCC, AC is more likely to form rich and homogeneous cribriform capillaries, with greater microvessel density, and the maturity of neovascularization formed by SCC is not as good as that of AC. Neovascularization is more likely to be broken or blocked due to the rapid growth of tumor tissues. Therefore, the uptake of iodine contrast agent in AC is higher than that in SCC. According to histopathological analysis, AC is mainly composed of glandular structure, which contains rich interstiitium, loose internal structure and the number of cells per volume is large, while SCC is mainly composed of cancer nests, keratinocytes, intercellular bridges and other structures. The internal structure is dense and there are fewer tumor cells per volume [24], so the extent of the penetration of contrast agent will also be different.

The spectral curve reflects the change of the CT value of the lesion under different keV. We can judge the properties, homology and difference of lesions by analyzing the spectral curve of lesions, and it also can reflect the absorption of the contrast agent in the lesion [25]. The results showed that the slope of different energy intervals are different, and the CT value of tissues will decrease with the increase of

energy, and the CT value of different energy levels representing the mass absorption coefficient of lesions at different energy levels [28]. In this study, the curve is steep in the range of 40 ~ 70 keV, and the curve is flat in the range of 70 ~ 100 keV. This is related to the larger the X absorption coefficient and the more X-ray attenuation at low energy. In this study, the slope of spectral curve between 40 and 70 keV was selected as the quantitative analysis index. The results showed that the $K_{70keV}$ of AC was higher than SCC during both AP and VP, and the difference was statistically significant, which was consistent with the research results of other scholars [25]. The slope of spectral curve reflects the intensity of lesion enhancement, so it is considered that AC absorbs more iodine contrast agents than SCC, and contrast agents enhance the difference of mass absorption coefficient between the two groups of lesions.

The effective atomic number (Zeff) can directly reflect the atomic number of the compound inside the lesion. If the X-ray attenuation coefficient of the atomic number of an element is the same as that of the compound, then the atomic number of the element is the atomic number of the substance [26]. According to this feature, the composition and properties of compounds can be identified [17], especially those with similar densities and CT values. Some studies have shown that the Zeff can accurately describe the histological characteristics of the lesion and distinguish the material components [24, 29, 30]. In this study, the Zeff of P-AC was greater than that of P-SCC during both AP and VP, and the difference was statistically significant. This may be due to the different pathological tissue types, the material composition and cell metabolic activity of the lesions are also different. And the Zeff with enhanced scan is related to the uptake dose of contrast agents by the lesions, which leads to the difference of Zeff between the P-AC and P-SCC [31].

According to ROC curve analysis, the combination of all parameters in AP and VP showed higher sensitivity (88%) and specificity (84%) Compared with the quantitative parameters alone during AP or VP in distinguishing P-SCC and P-AC, and the diagnostic efficiency of the AP is higher than that of VP. Zhang et al. [7] who found that quantitative parameters in VP had greater significance in differentiating SCC and AC than in AP. However, Jia et al. [25] found that the quantitative parameters of the two phases had no significant difference in distinguishing SCC from AC. The difference between the above studies may be due to the fact that each quantitative parameter is related to the uptake of contrast agents by the lesions, which may be affected by the dose of contrast agent, the enhanced scanning time of each phase, and the patient's hemodynamic status, resulting in different Research results [31]. It may also be due to the samples included in these studies is small or the lack of distinction between lung cancer types, such as peripheral and central squamous cell carcinomas, which may affect the results between different parameters. At present, our study with the largest sample to distinguish P-AC and P-SCC. Therefore, our results are more accurate and generalized.

There are several limitations in this study. First, this study was a retrospective study, which may lead to sampling bias. Secondly, this study focuses on differentiating P-SCC and P-AC, and other histological subtypes of lung cancer were not included. In future studies, more lung cancer subtypes will be included to draw broader conclusions. Finally, in order to reduce the radiation dose, the patients were not scanned

for the delayed phase. Therefore, more studies are needed to confirm whether the quantitative parameters during the delay period can differentiate P-SCC and P-AC.

## Conclusions

The quantitative parameters of spectral CT have important value in the differentiating P-SCC and P-AC, and can provide certain imaging basis for the choice of treatment and prognosis of lung cancer patients.

## Declarations

**Ethics approval and consent to participate:** The Ethics Committee of the Second Hospital of Lanzhou University (Lanzhou, China) approved the use of patient materials in this study.

**Availability of data and materials:** The datasets used and/or analysed during the current study are available from the corresponding author on reasonable request.

**Competing interests:** The authors declare that they have no competing interests.

**Funding:** This work was supported by the Talent Innovation and Entrepreneurship Project of Lanzhou (grant number 2016-RC-58); Open Fund project of Key Laboratory of Medical Imaging of Gansu Province (grant number GSYX202010).

**Acknowledgements:** Not applicable.

## References

1. Freddie B, Ferlay J, Isabelle S, et al. Global cancer statistics 2018: GLOBOCAN estimates of incidence and mortality worldwide for 36 cancers in 185 countries. 2018.
2. Meng F, Zhang L, Ren Y, Ma QJJoCP. The genomic alterations of lung adenocarcinoma and lung squamous cell carcinoma can explain the differences of their overall survival rates. 2018.
3. Herbst R, Heymach J, Lippman SJTNEjom. Lung cancer. 2008;359(13):1367–80.
4. Nagai KJJJoCO. Differences between squamous cell carcinoma and adenocarcinoma of the lung: are adenocarcinoma and squamous cell carcinoma prognostically equal? 2012;42(3):189 – 95.
5. Xiong S, Zhang Z, Mei L, et al. Differential expression of sonic hedgehog in lung adenocarcinoma and lung squamous cell carcinoma. 2019;66(5):839–46.
6. Beslic S, Zukic F, Milisic SJR. Oncology. Percutaneous transthoracic CT guided biopsies of lung lesions; fine needle aspiration biopsy versus core biopsy. 2012;46(1):19–22.
7. Zhang Z, Zou H, Yuan A, Jiang F, Gong LJAR. A Single Enhanced Dual-Energy CT Scan May Distinguish Lung Squamous Cell Carcinoma From Adenocarcinoma During the Venous phase. 2019;27(5).

8. Rios Velazquez E, Parmar C, Liu Y, Coroller T, Cruz G, Stringfield O, et al. Somatic Mutations Drive Distinct Imaging Phenotypes in Lung Cancer. 2017;77(14):3922–30.
9. Zhang Y, Hu CJAi I, mmAopotSfA. WIF-1 and Ihh Expression and Clinical Significance in Patients With Lung Squamous Cell Carcinoma and Adenocarcinoma. 2016:1.
10. Yue J, Chen J, Zhou F, Hu Y, Li M, Wu Q, et al. CT-pathologic correlation in lung adenocarcinoma and squamous cell carcinoma. 2018;97(50):e13362.
11. Shin B, Shin S, Chung M, Lee H, Koh W, Kim H, et al. Different histological subtypes of peripheral lung cancer based on emphysema distribution in patients with both airflow limitation and CT-determined emphysema. 2017;104:106–10.
12. Kunihiro Y, Kobayashi T, Tanaka N, Matsumoto T, Okada M, Kamiya M, et al. High-resolution CT findings of primary lung cancer with cavitation: a comparison between adenocarcinoma and squamous cell carcinoma. 2016;71(11):1126–31.
13. Jiang B, Takashima S, Miyake C, Hakucho T, Takahashi Y, Morimoto D, et al. Thin-section CT findings in peripheral lung cancer of 3 cm or smaller: are there any characteristic features for predicting tumor histology or do they depend only on tumor size? 2014;55(3):302-8.
14. Kim E, Kim Y, Park I, Ahn H, Cho E, Jeong Y, et al. Evaluation of sarcopenia in small-cell lung cancer patients by routine chest CT. 2016;24(11):4721–6.
15. Phillips M, Bauer T, Cataneo R, Lebauer C, Mundada M, Pass H, et al. Blinded Validation of Breath Biomarkers of Lung Cancer, a Potential Ancillary to Chest. CT Screening. 2015;10(12):e0142484.
16. McCollough C, Leng S, Yu L, Fletcher JJR. Dual- and Multi-Energy CT: Principles, Technical Approaches, and Clinical Applications. 2015;276(3):637–53.
17. So A. Nicolaou SJKjor. Spectral Computed Tomography: Fundamental Principles and Recent Developments. 2020.
18. Sudarski S, Hagelstein C, Weis M, Msc, Schoenberg SO, Apfaltrer PJEJoR. Dual-energy snap-shot perfusion CT in suspect pulmonary nodules and masses and for lung cancer staging. 2015.
19. Zhang G, Cao Y, Zhang J, Zhao Z, Zhang W, Huang L, et al. Focal organizing pneumonia in patients: differentiation from solitary bronchioloalveolar carcinoma using dual-energy spectral computed tomography.12(7).
20. Sandler A, Gray R, Perry MC, Brahmer J, Johnson DHJNEJoM. Paclitaxel–Carboplatin Alone or with Bevacizumab for Non–Small-Cell. Lung Cancer. 2007;355(24):2542–50.
21. Giorgio Vittorio S. Phase III study comparing cisplatin plus gemcitabine with cisplatin plus pemetrexed in chemotherapy-naive patients with advanced-stage non-small-cell lung cancer. %J Journal of clinical oncology: official journal of the American Society of Clinical Oncology. 2008;21:26.
22. Wang G, Zhang C, Li M, Deng K, Li WJJoCAT. Preliminary Application of High-Definition Computed Tomographic Gemstone Spectral Imaging in Lung Cancer. 2014;38(1):77–81.

23. Hong S, Rom, Hur, Jin M, et al. Predictive factors for treatment response using dual-energy computed tomography in patients with advanced lung adenocarcinoma. 2018.
24. Jia X, Sun, radiology JJC. CT spectral parameters and serum tumour markers to differentiate histological types of cancer histology. 2018.
25. Jia Y, Xiao X, Sun Q, Jiang HJM. Gemstone spectral imaging in lung cancer: A preliminary study. 2018;97(29).
26. Yuan A, Yu CJ, Kuo SH, Chen WJ, Lin FY, Luh KT, et al. Vascular Endothelial Growth Factor 189 mRNA Isoform Expression Specifically Correlates With Tumor Angiogenesis, Patient Survival, and Postoperative Relapse in Non–Small-Cell. Lung Cancer. 2001;19(2):432–41.
27. Yazdani S, Miki Y, Tamaki K, Ono K, Iwabuchi E, Abe K, et al. Proliferation and maturation of intratumoral blood vessels in non-small cell lung cancer. 2013;44(8):1586–96.
28. Wang Q, Shi G, Qi X, Fan X, Wang LJEJoR. Quantitative analysis of the dual-energy CT virtual spectral curve for focal liver lesions characterization. 2014;83(10):1759–64.
29. González-Pérez V, Arana E, Barrios M, Bartrés A, Cruz J, Montero R, et al. Differentiation of benign and malignant lung lesions. Dual-Energy Computed Tomography findings. 2016;85(10):1765–72.
30. The Value of Nonenhanced Single. -Source Dual-Energy CT for Differentiating Metastases From Adenoma in Adrenal Glands %J. Academic Radiology. 2015;22(7):834–9.
31. Q Z. [Comparative imaging study of mediastinal lymph node from pre-surgery dual energy CT < i > versus</i > post-surgeron verifications in non-small cell lung cancer patients]. %J Beijing da xue xue bao. Yi xue ban = Journal of Peking University. Health sciences. 2020;4(52).

# Figures

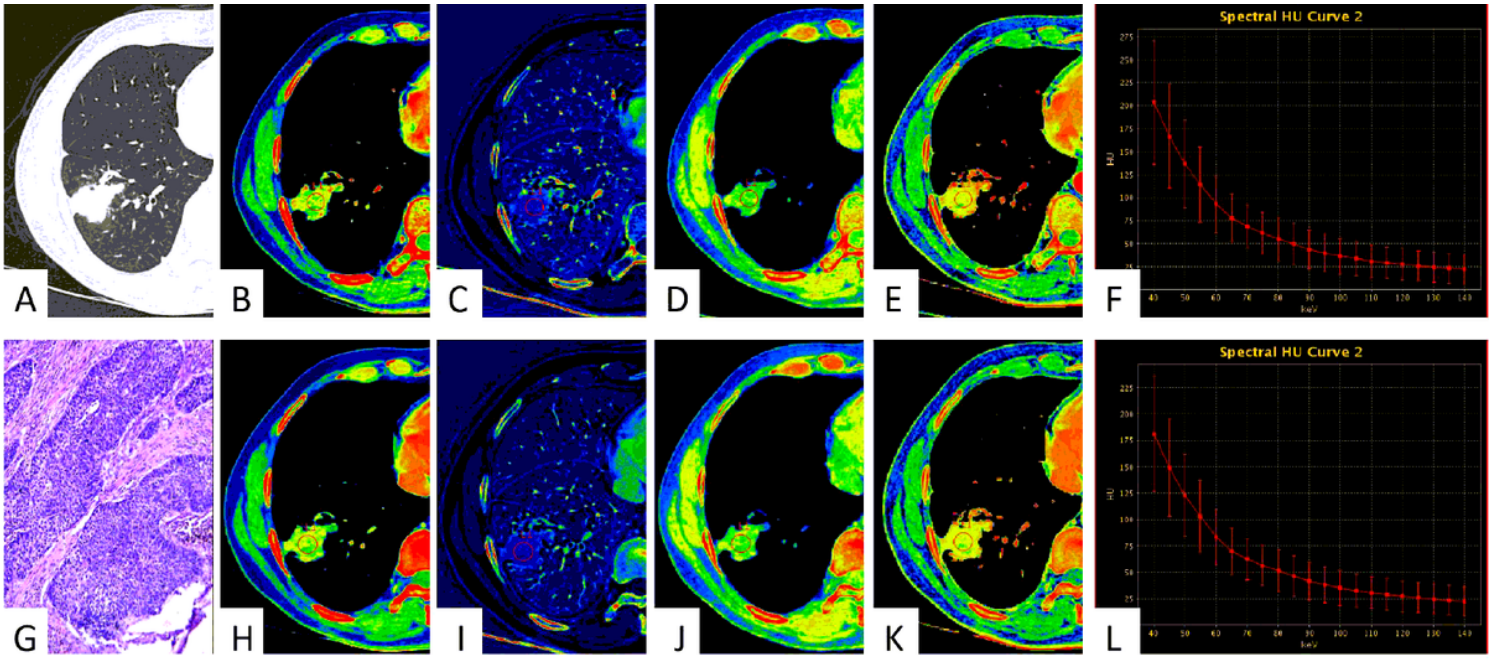


**Figure 1**

Spectral computed tomography (CT) images and histopathological section from a 61-year-old woman with peripheral squamous cell carcinoma (P-SCC). a Lung window. b, h monochromatic CT image acquired at 70 keV during the arterial phase (AP, 69.32 HU) and venous phase (VP, 63.83 HU). c, i The iodine-based material decomposition image with iodine concentrations (IC) of 23.62 100ug/cm3 during the AP and 20.74 100ug/cm3 during the VP. d, j The water-based material decomposition image with water concentrations (WC) of 1,009.73 mg/cm3 during the AP and 1,012.27 mg/cm3 during the VP. e, k The effective atomic numbers (Zeff) were 8.78 during the AP and 8.70 during the VP. f, l The spectral curve is shown during the AP and during the VP. g Hematoxylin and eosin staining (×100).

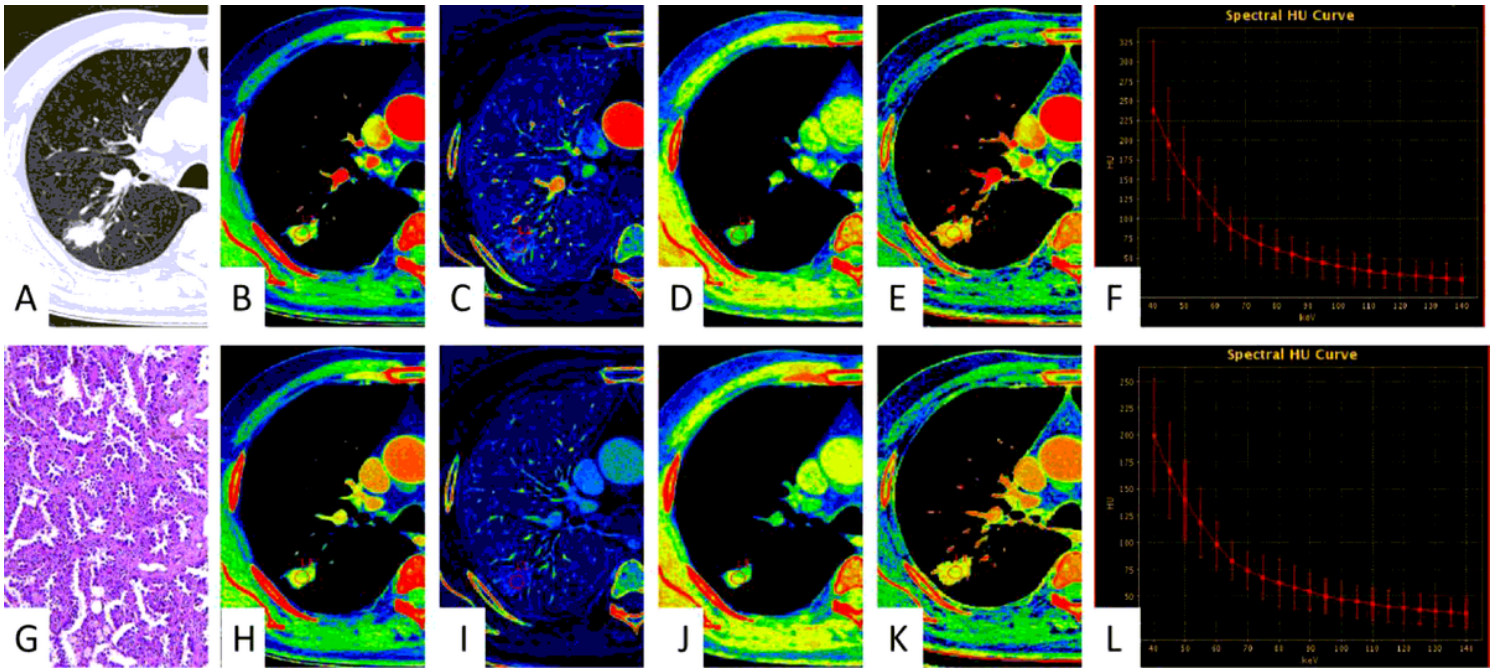


**Figure 2**

Spectral computed tomography (CT) images and histopathological section from a 62-year-old man with peripheral lung adenocarcinoma (P-AC). a Lung window. b, h monochromatic CT image acquired at 70 keV during the arterial phase (AP, 75.98 HU) and venous phase (VP, 74.5 HU). c, i The iodine-based material decomposition image with iodine concentrations (IC) of 27.93 100ug/cm3 during the AP and 21.55 100ug/cm3 during the VP. d, j The water-based material decomposition image with water concentrations (WC) of 1,007.95 mg/cm3 during the AP and 1,023.07 mg/cm3 during the VP. e, k The effective atomic numbers (Zeff) were 9.17 during the AP and 8.85 during the VP. f, l The spectral curve is shown during the AP and during the VP. g Hematoxylin and eosin staining (×200).

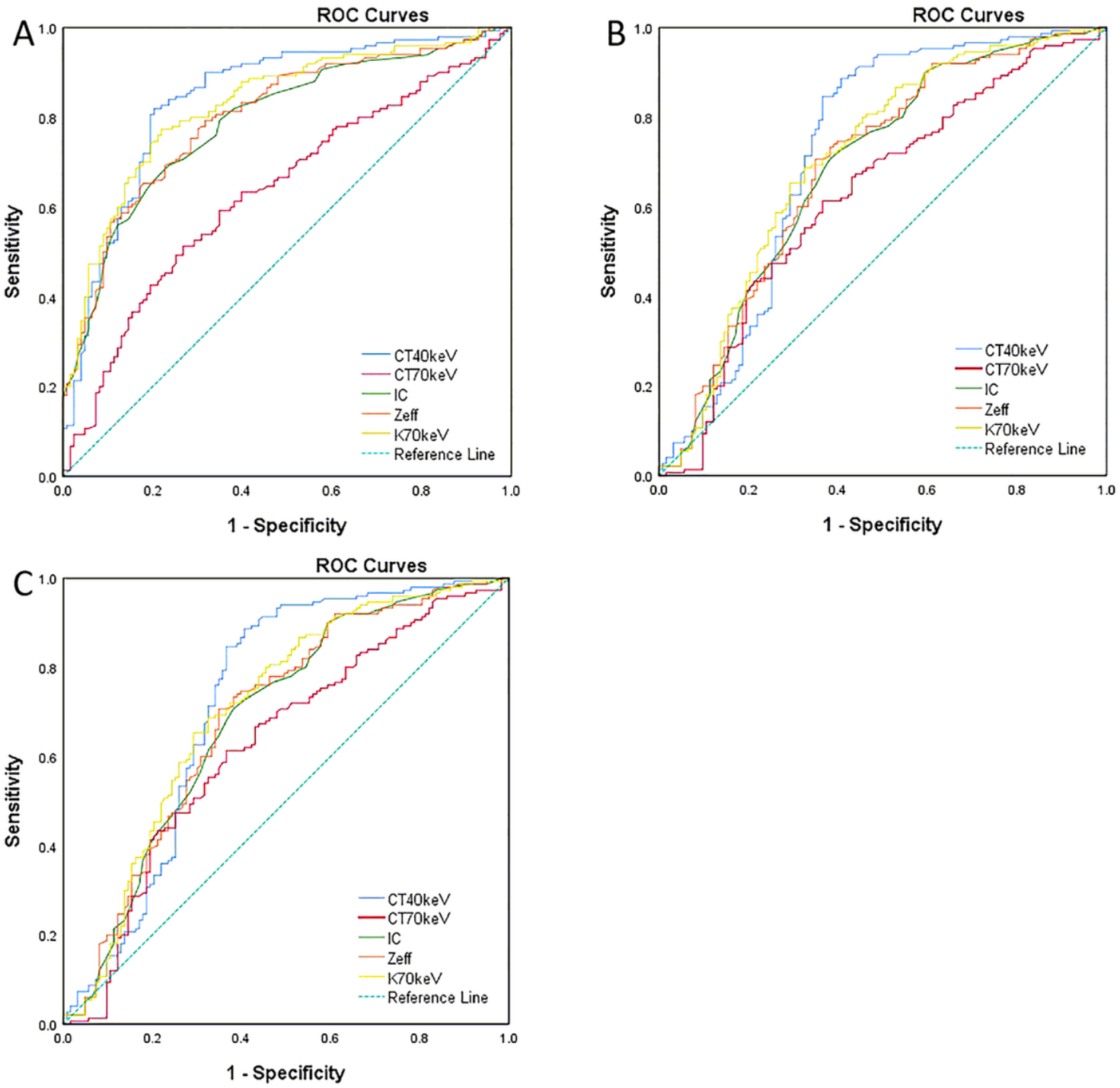


## Figure 3

The Receiver operating characteristic (ROC) curve of all parameters. A. The CT40keV, CT70keV, K70keV, iodine concentration (IC) and effective atomic number (Zeff) to differentiate P-SCC and P-AC in arterial phase (AP); B. The CT40keV, CT70keV, K70keV, IC and Zeff to differentiate P-SCC and P-AC in venous phase (VP); C. The combination of quantitative parameters in the arterial phase (AP-all), the combination of quantitative parameters in the venous phase (VP-all), and the combination of all quantitative parameters in the AP and VP (AP-all +VP-all).